ERJ Express. Published on July 26, 2006 as doi: 10.1183/09031936.06.00012405

AIRWAY DIMENSIONS MEASURED FROM MICRO COMPUTED TOMOGRAPHY (CT) AND HIGH RESOLUTION CT

Jessica R. Dame Carroll[1,2,4], Aneal Chandra[1,2,4], Allan S. Jones[3], Norbert Berend[1,2,4], John S. Magnussen[1,6] & Gregory G. King[1,2,4,5]

1. The Woolcock Institute of Medical Research, Sydney 2050, Australia.
2. The Cooperative Research Centre (CRC) for Asthma, Sydney 2050, Australia.
3. The Key Centre for Microscopy and Microanalysis, the University of Sydney 2006, Australia.
4. The University of Sydney, Sydney 2006, Australia.
5. Department of Respiratory Medicine, Royal North Shore Hospital, St. Leonards 2065, Australia.
6. Department of Radiology, Royal Prince Alfred Hospital, Camperdown 2050, Australia.

Correspondence:

Gregory G. King
Woolcock Institute of Medical Research
University of Sydney 2006
Australia
Phone: (61 +2) 9926 6265
Fax: (61 +2) 9906 6391
email: ggk@woolcock.org.au

Support: This work was supported by the CRC for Asthma (Project 12b) and National Health and Medical Research Council Project Grant #153839.

Running head: Micro CT measurements of airways.

Subject category number: 47

Abstract word count: 197

Body word count: 4355
Keywords: Image Processing, Computer-Assisted; Phantoms, Imaging; Validation Studies

Abstract

Volume averaging results in over- and underestimation of airway dimensions measured from High-resolution CT (HRCT). We calibrated computerized measurements of airway dimensions from HRCT against a novel 3-dimensional micro-CT standard, which has a fifty-fold greater resolution, as well as with traditional morphometry.

Inflation-fixed porcine lung cubes were scanned by HRCT and micro-CT. 59 lumen area (Ai), 30 wall area (Aaw) and 11 lumen volume (Vi) measurements were made. Ai was measured from the cut surface of 11 airways by morphometry. Airways in scanned images were matched using branching points. After calibration, the errors of Ai, Aaw and Vi HRCT measurements were determined.

We found a systematic, size-dependent under-estimation of Ai and overestimation of Aaw from HRCT measurements which we used to calibrate our HRCT measurement algorithm. The 95% limits of agreement of subsequent measurements were $\pm 3.2 mm^2$ for Ai, $\pm 4.3 mm^2$ for Aaw, and $\pm 11.2 mm^3$ for Vi with no systematic error. Morphometric measurements agreed with micro-CT ($\pm 2.5 mm^2$) without systematic error.

Micro-CT image data from inflation fixed airways can be used as calibration standards for three-dimensional Vi measurements for HRCT, while morphometry is acceptable for two-dimensional measurements. This image dataset could be used to validate other developmental 3-dimensional segmentation algorithms.

Introduction

Due to multi-detector technology, image data obtained for High-resolution Computed Tomography (HRCT) are currently routinely acquired volumetrically and have been used for quantitative image analysis of airways and lung tissue in many studies (1-9). Direct measurements of airway structures can be made from HRCT image data making it useful for studying asthma, cystic fibrosis and chronic obstructive pulmonary disease. Airway dimensions have been measured from HRCT image data using customized computer analysis algorithms which have been validated using airway phantoms of known dimensions constructed from non-animal materials such as plexiglass and sweet potatoes (4, 8, 10-12). In these studies the measurements were made from planimetric measurements of a cut surface of the phantom and it was therefore reasonably assumed that the dimensions would be completely uniform along the length of the airway phantom and that the orientation in the z-axis of the scanning plane could be accurately controlled.

Validation of airway measurement algorithms advanced further with the use of explanted animal lungs as calibration standards. Porcine lungs that were wet-fixed with formalin (13) have been used and we have previously used formalin inflation-fixed porcine lungs (8) for validation. The use of liquid-fixed resected human lung tissue for validation has also recently been described (13). Explanted lung preparations are more suitable than artificial phantoms for validation because they closely approximate the range of tissue densities and dimensions, and the complex structure of lung tissues *in vivo* such as mucosal folding and irregularities in airways, which are not present in artificial phantoms. This difference compared with artificial material phantoms is, in turn, associated with different estimates of measurement errors for HRCT (8). HRCT measurements are affected by volume averaging, particularly in the scanner's z-axis due to the complexity of the structures, range of tissue densities, inability to control airway orientation in the z-axis during scanning and it being the longest dimension of the voxel (see Figure 1). To calibrate 3-D HRCT measurements of airways, we required a 3-D standard of known dimensions so that the effects of volume averaging would be accounted for in the calibration process, while also allowing measurement of precision and accuracy of the HRCT method. Because morphometry is 2-D, there is by definition, no volume averaging in the z-axis affecting this measurement.

Micro-CT is currently used for studying the 3-D structure of a wide range of small objects in microscopic detail with image data consisting of cubic voxels as small as 2x2x2 μm, but its use in lung has not been widely explored. Micro-CT resolution is almost two orders of magnitude greater than HRCT in which voxel size is typically 0.5 x 0.5 x1 mm. The resolution of micro-CT should allow airways measurements of similar or greater accuracy to morphometry but that are three-dimensional, which would allow validation of 3-D segmentation algorithms used to measure airway dimensions *in vivo* (see Figure 2). The aim of the study was to validate micro-CT against the current calibration standard of morphometry of the cut surface of the lung and calliper measurement of cylindrical rods. Our second aim was to use measurements of lumen area (Ai) and wall area (Aaw) of inflation fixed porcine airways from micro-CT images to calibrate our HRCT airway segmentation algorithm. Finally, we aimed to then assess the precision and accuracy of 3-D measurements of airway volume (Vi) of the calibrated segmentation.

Methods

To validate micro-CT as the calibration standard for our HRCT airway segmentation algorithm we compared Micro-CT diameter measurements of various sized cylindrical rods made of plastic and wood to calliper measurements. We also compared Ai measurements from a single micro-CT image of the cut surface of inflation fixed porcine lung to the current gold standard of tissue morphometry.(8, 14). Using micro-CT measurements of Ai and Aaw, we calibrated our current segmentation algorithm for unbiased Ai and Aaw measurements from HRCT and then determined the precision of Ai, Aaw and Vi measurements of our calibrated algorithm (95% limits of agreement). Finally, we examined the agreement between our calibrated Ai measurements from the cut surface of the lung from HRCT with morphometric measurements. (See figure 3)

Lung preparation and fixation

The lungs were fixed in inflation with formalin (8) using a modification of a method described by Weibel and Vidone (15). The lungs were obtained from a local butcher and were fixed between 12-24 hours after being removed from the animal. Formalin steam was passed into the lung and negative pressure was applied to the exterior of the lung to fix the lung in inflation at an approximate inflation pressure of 25 cmH_20 (see figure 4). Fixation time was approximately 2 hours, depending on the size of the lung specimen.

After fixation and cooling to room temperature, the lung was then scanned by HRCT and airways of interest were identified. The lung was then cut into 2cm cubes in a plane that was approximately perpendicular to the z-axis of the airways of interest. The cut surfaces of the lung cubes were then photographed. Finally, these 2cm lung cubes were then wrapped in plastic wrap and coated in paraffin for protection (Paraplast, Tyco Healthcare, USA).

Digital imaging of the lung

Immediately prior to being wrapped and coated with paraffin, the cut surface of the lung cubes were photographed through a dissecting microscope with a 3.34 mega pixel digital camera (Nikon Coolpix 995 with a Relay Lens (MDC2)) and images were saved as 1024 x1024 bitmap files. After the lung cubes were wrapped and coated in paraffin they were then scanned in both the HRCT (GE 4-slice Lightspeed, GE Medical Systems, Minneapolis) and SkyScan 1072 micro-CT desktop system (SKYSCAN, Aartselaar, Belgium). HRCT settings were 100kV and 100mAs at a slice thickness of 1.25mm and a pitch of one in helical mode. Images were reconstructed using the GE high spatial frequency 'Bone' algorithm at a field of view (FOV) of 18cm, which yielded a voxel size of 0.35x0.35x1.25 mm. Images were archived in DICOM format onto CD for later analyses. Micro-CT settings were 100kV and 100mAs at a slice thickness of 19μm and a FOV of 19mm, which yielded a voxel size of 19x19x19μm. Each cube was scanned every 0.23 degrees as it rotated around its vertical axis until it had rotated 180 degrees, at an exposure time of 0.9 seconds per scan. Images were reconstructed using the ConeRec software provided by SkyScan. Reconstructed image data were archived in Bitmap format onto DVD for later analyses.

Image Analysis

A single operator (JDC) measured lumen and wall areas of airways visible in cross section in the digital photographic bitmap images of the cut surface of the lung, by manually tracing the inner and outer edges of the airway wall with the computer mouse using ImageJ software (National Institute of Mental Health, Bethesda, Maryland, USA). Each airway was traced twice to assess for measurement repeatability, and the average of the two tracings was used for analysis.

Ai and Aaw measurements were made directly from the HRCT image data (DICOM format) using an in-house, custom-written software program for Micorsoft Windows operating systems. The HRCT lung images were displayed on the program screen and the airway of interest was identified manually. The centroid of the airway was automatically identified, from which 20 radial spikes were created. The inner and outer edges of the airway wall were defined as the point along the radial spikes at which the greatest rate of change in density occurred, i.e. from air to soft tissue.

We measured Ai and Aaw from micro-CT bitmap images by the same method as for morphometry, i.e. tracing the inner and outer edges of the airway wall using the computer mouse in the ImageJ software. The lumen and wall areas were calculated as the product of the pixel size (19x19 μm^2) and the number of voxels within the traced border. A single operator (JDC) traced each airway border twice, and the average of both measurements was used for analysis. For comparisons of micro-CT and morphometry, we measured all airways that were visible in both the micro-CT FOV and the digital photographs of the cut surface of the lung specimens. This resulted in a range of airway sizes comparable to what we have measured in a previous HRCT study of asthmatic and normal airways. (16)

For comparisons between HRCT and micro-CT, airways were matched using airway branch points as anatomical markers. Since the HRCT slice thickness of 1.25mm was over sixty times thicker than the micro-CT slice thickness of 19μm, we used every thirtieth micro-CT image which resulted in an effective slice thickness of 0.57 mm. To calibrate Ai measurements from HRCT, the average of three consecutive Ai and Aaw measurements from micro-CT images which covered a thickness of 1.14 mm, was compared with each corresponding HRCT slice of thickness 1.25 mm. Micro-CT and HRCT measurements of airway volume (Vi) were calculated as the sum of all lumen voxels in the airway. Voxel dimensions for micro-CT were 19x19x570 μm since the interslice gap was every thirtieth image (30 slices x 19μm = 570μm). The voxel dimensions for HRCT were 0.35 x 0.35 x 1.25mm since slice thickness was 1.25 mm.

Statistical analyses

All data are shown as mean ±95% confidence interval unless otherwise specified.

Intra-observer variation

The intra-observer variation in 72 calliper measurements of the rods, in Ai and √Ai measurements from morphometry in 29 airways, and in Ai measurements from micro-CT in 30 airways, were determined by the methods of Bland and Altman and expressed as the repeatability, being the 95% limits of agreement (17) (18)

Agreement between imaging methods

The agreement of the Ai and Aaw measurements made by both the semi-automated HRCT algorithm and the micro-CT technique was calculated by the method of Bland & Altman and expressed as the 95% limits of agreement, being $t_{0.05}$ x standard deviation of the differences between micro-CT and HRCT measurements where $t_{0.05}$ is the critical t-value corresponding to the sample size at the 0.05 level of significance . Agreement between micro-CT measurements and calliper measurements of the artificial material rods was similarly calculated.

Calibration of HRCT measurements

The relationship between Ai and Aaw measurements from micro-CT and HRCT was used as a calibration factor for the HRCT measurements and the subsequent 95% limits of agreement was re-calculated as above.

Results

Calliper measurements

The measurements made by micro-CT were validated against 72 calliper measurements of cylindrical rods made of artificial materials with diameters between 0.8mm and 9.8mm. The intra-operator repeatability of the calliper measurements of the rods was ±0.21mm and was independent of diameter. However, as expected when expressed as percent error, it was greater for smaller rods. The mean difference between micro-CT and calliper measurements of diameter was 0.03±0.03mm (p=0.14) and the 95% limits of agreement were ±0.285 mm. Thus, there was no systematic error in micro-CT measurements.

Morphometry vs Micro-CT of Airways

There was good agreement between Ai measurements of 11 airways from the digital photographs of the cut lung surface compared with measurements from micro-CT (Figure 5). Within the range of airway sizes we were able to study (0.9 – 36.4-mm^2), the mean difference was 0.14±0.6mm^2 (p=0.69) and were independent of airway size; the 95% limits of agreement were ± 2.5mm^2. The intra-operator (JDC) repeatability of Ai and √Ai measurements from morphometry was ±0.555mm^2 or 3.1% and ±0.066mm or 1.6%, respectively. The intra-operator repeatability of Ai measurements from micro-CT was ±0.557mm^2 or 1.9%.

Micro-CT vs HRCT of Airways

Fifty-nine Ai measurements from micro-CT and HRCT were compared. The mean Ai from micro-CT was 24.1 ± 5.7mm^2 (idealized diameter 5.1 ± 0.5mm) and ranged from 1.7 to 80.9 mm^2. There was a systematic and size-dependent underestimation of Ai when measured from HRCT which was linear in nature (Figure 6a). From a plot of micro-CT Ai and HRCT Ai (not shown, r^2 = 0.96, p <0.0001) we found the difference between the Ai measured from both methods fit the following equation: *HRCT Ai = 0.7224 x micro-CT Ai - 1.7241*. After this equation, or calibration factor, was applied to all HRCT Ai measurements, the 95% limits of agreement of Ai measurement were ± 3.2mm^2 (Figure 6c). When expressed as percentage errors (see Figures 6b and 6d), the errors were expectedly larger for smaller airways. The percentage error was greatest in airways with an Ai <10mm^2 (internal diameter 3.5mm).

Thirty airway wall area measurements from micro-CT and HRCT were compared (mean Ai 29.4 ± 9.6mm^2, idealized diameter 6.5 ± 1.0mm). Airways with an Aaw <10mm^2 could not be segmented for wall area reliably with our segmentation algorithm, and were therefore excluded from this analysis. The excluded airways had a corresponding Ai of less than 5mm^2, and an idealized diameter of less than 2.5mm. The overestimation of the HRCT Aaw measurement was size-dependent and linear in nature (Figure 7a). From a plot of micro-CT Aaw and HRCT Aaw (not shown, $r^2 = 0.97$, $p<0.0001$), we found the difference in Aaw to fit the following equation: *HRCT Aaw = 0.8872 x micro-CT Aaw + 8.8611*. After calibration of the HRCT Aaw measurements, the 95% limits of agreement of Aaw measurements were ±4.3mm^2 (Figure 7c). The errors were again larger for smaller airways when expressed as percentage errors (Figures 7b and 7d). The percentage error was greatest in airways with an Aaw of <10mm^2.

Airway volume was measured using the calibrated segmentation algorithm for all airways that had at least three consecutive HRCT images in which segmentation could be done. Airway lumen volume was calculated as the product of voxel volume (0.35x0.35x1.25mm) and the number of voxels within the lumen from all contiguous slices along the airway volume. Volume measurements from HRCT images from 11 airways using the calibrated measurements agreed closely with micro-CT Vi measurements with no systematic error or size-dependence (Figure 8a). The 95% limits of agreement were ±11.2mm^3. Again, when errors were expressed as a percentage of airway volume, the relative errors were larger for smaller airways (Figure 8b).

Discussion

In this study we obtained two-dimensional and three-dimensional measurements of the airway lumen from micro-CT images of explanted lung tissue to serve as calibration standards. We used an inflation fixation that kept the tissue at a similar density to what it would have been *in vivo*, then undertook morphometry, HRCT scanning and micro-CT scanning of the same tissue. By using micro-CT, we overcame the previous limitation of having only two-dimensional calibration standard measurements (i.e. lumen area) of explanted airways. We found that our Ai segmentation method for HRCT data resulted in significant underestimation when compared to the calibration standard measurements, and that the measurement error was predictable, being size-dependent in a linear fashion. We also found that our segmentation algorithm for HRCT resulted in a linear, size-dependent overestimation of Aaw. The calibration of our computerized segmentation algorithm resulted in Ai and Aaw measurements from HRCT that were free of systematic errors and allowed determination of the overall precision of our measurement tool. The close agreement and lack of systematic error between micro-CT and morphometric measurements of Ai suggest that micro-CT measurements do not suffer any significant volume averaging. By validating our ray-casting segmentation for HRCT against micro-CT the Vi measurements were accurate having relatively small and unbiased errors.

There are several possible sources of errors in airway measurements from HRCT image data and these include volume averaging (which can be exacerbated by more acute angles of airway orientation relative to the scanning plane); the scanners' point spread functions and reconstruction algorithms; and the lumen segmentation methods (19). It is possible to measure the angles of orientation of airways from volumetric HRCT data to correct for volume averaging(20), which may potentially reduce variation in HRCT measurements. We were unable to do this with the current iteration of our analysis algorithm but it needs to be addressed in future studies. It is likely that these sources of error may differ between manufacturers and models of HRCT machines. Therefore, it

may be useful to examine the variations in CT image data arising from clinical CT scanners produced by different manufacturers, as well as that arising from different reconstruction algorithms. The magnitude of the variation is not known nor whether it is clinically significant, although it is common for serial chest CT scans done for monitoring disease to be done on different scanners.

Manual outlining of airway lumen borders on micro-CT image data might have been an additional source of error, which we think is likely to be very small. This is because of the very small errors in measurements of diameter obtained from the cylindrical rods which are an order of magnitude less than the errors introduced through HRCT image acquisition and analysis. Measurements of Ai, Aaw and Vi made from micro-CT were unaffected by window settings because of the great spatial resolution and the great contrast at the lumen interface. It is interesting that the limits of agreement between micro-CT and surface morphometry ($\pm 2.5 mm^2$) were similar to the agreement between micro-CT and HRCT ($\pm 3.2 mm^2$). The disagreement between micro-CT and surface morphometry may be due to the reconstruction plane of micro-CT being slightly out of alignment with the cut surface of the lung which was photographed. The implication is that similar errors are likely to have occurred when comparing micro-CT with HRCT and also suggests that the comparison method could be improved in the future by using a three-dimensional registration process to remove this potential source of error. It should also be noted that in some cases, the airways tended to taper towards the surface of the lung cubes with the airway reaching its largest diameter toward the centre of the lung cube. These airways were not included in the comparison between micro-CT and morphometry, because they were not visible on the cut surface of the lung.

Volume averaging is the factor most likely accounting for the bulk of the errors in Ai measurements. The effects of volume averaging on apparent Ais are likely to be greatest in the z-axis in HRCT, because the z-dimension of the HRCT voxel (1.25 mm) is almost four times longer than the x and y dimensions (0.35 mm). This is relevant because airways are usually not parallel to the z-axis in human HRCT studies, nor were they in our current study. As a result, the effects of volume averaging and hence the magnitude of the underestimation of lumen area are greater as airway size decreases and the angle of orientation increases (see Figure 1) (8, 19, 21). The use of micro-CT for calibration allowed us to account for the effects of volume averaging, which we would not have been able to do with two-dimensional measurements. Furthermore, when spiral CT is used, rather than conventional axial high-resolution CT, there is a blurring of structures in the z-axis due to the continuous movement of patients through the rotating tube. Finally, we measured Ai, Aaw and Vi from HRCT image data which are measured in Hounsfield Units, a measure of tissue density(19). They are therefore unaffected by window level or width settings, which can affect visual analyses of photographed images (11, 22).

We found that the lower limit of airway size on which lumen measurements could be made with accurately, in terms of percent errors, was approximately $10 mm^2$, which corresponds to an idealized internal diameter of 3.5mm in our dataset, which corresponds to 4^{th} generation or segmental airways. Airway wall area measurements were accurate in airways with wall areas greater than approximately $10 mm^2$, which corresponds to airways with internal diameters of approximately 2.5mm, which corresponds to 5^{th} generation or sub-segmental airways. The implication is that greater numbers of airways need to be measured when looking at any percent changes in Ai or Aaw associated with interventions, for airways smaller than those specified above. However, there is greater power if absolute changes in either Ai or Aaw are being measured. It is essential to be able to correct or calibrate the measurements made from HRCT, and to know the accuracy of the subsequent calibrated measurements so that studies that are designed to look for changes in airway dimensions are powered appropriately. For instance, because we found that even after calibration, smaller airways continued

to have large errors associated with them when expressed as a percentage of airway size, a much larger number of small airways would need to be studied in patients to detect a real effect of an intervention on smaller airway dimensions than in larger airways where the error as a percentage of total area is much smaller.

We used one airway segmentation method for HRCT, although there are many different airway analysis algorithms, all of which are based on slightly different segmentation criteria (1, 3-8, 21). We used the point at which the density change over two pixels was maximal along the radial spike, while others have used the more common 'full width at half-max' method. Our method is likely to result in a greater underestimation of the lumen, but we chose this because it appeared to reliably segment the lumen even in small airways. Another possible factor is the number of radial spikes used in the segmentation. The ideal number may vary depending on the edge detection method and is worthy of further study. Such systematic errors relating to a particular methodology of finding the airway lumen edge can be corrected by comparison with calibration standards generated by studies such as the present one. The precision of different segmentation methods can then be meaningfully compared. The dataset of HRCT airway images could be used in the future to compare and possibly standardize measurements made by the different segmentation algorithms. Given the increasing likelihood that computerized segmentation will be used routinely in clinical practice to measure airway dimensions, documentation of the differences in Ai and Aaw measurements associated with different segmentation methods needs to be done using calibration standards in follow-up studies.

The formalin steam fixation method did not significantly alter the lung density, which makes this validation method likely to be more accurate and relevant to *in vivo* lung imaging compared with validation with artificial material phantoms. Lung density pre- and post-fixation was 0.34 gm/ml and 0.38 gm/ml, respectively. We compared the tissue density of the formalin fixed pig lung with human *in vivo* lung as measured by HRCT and found them to be similar. The lung cubes were very delicate and needed to be handled extremely gently as they were moist and were not completely stiff. We used a very sharp and thin knife to slice the lung, and we did notice some slight distortion of the parenchyma at the site of slicing in our lung cubes. Since all of the analysis was performed after slicing, the effect of the small distortions at the sliced edge was constant across imaging techniques and not considered an important issue. We considered wet fixation (commonly used for excised lungs in which formalin solution is pumped into the lung or lobe) to be unsuitable for this validation, because it results in fluid-filled alveoli, thereby altering mean lung density, as well as introducing additional fluid into the airway lining. Dry fixation was similarly considered to be unsuitable by causing desiccation of the lung. Therefore, our use of the calibration standard described in this manuscript gives a more 'real life' measure of artefacts in airway appearance and measurement that would be occurring in HRCT scans of human subjects. Another strength of this study is that the micro-CT, morphometry and HRCT were performed after fixation, which allowed us to determine measurement errors that were associated with image analysis since there could be no errors due to fixation artefacts.

HRCT provides the unique opportunity to make direct measurements on airways *in vivo* over time to monitor the response of airways to treatment or other stimuli. It is essential that airway measurements are accurate and that the accuracy of the measurements is independent of airway size since an airway that is reduced in size due to moderate or severe increases in smooth muscle tone, inflammation or wall thickening, may likely experience large changes in lumen size if the inflammation and bronchoconstriction resolve. If the accuracy of the measurements is largely size-dependent, then the magnitude of the change in airway dimensions will be masked. It is well accepted that HRCT measurements of lumen area tend to underestimate actual lumen area in a size

dependent fashion such that the absolute error increases as airway size increases, and HRCT measurements of airway wall tend to overestimate actual airway wall dimensions in the same size-dependent fashion(8). Therefore, if a patient was scanned during an acute exacerbation of asthma while his airways were inflamed and constricted, then scanned again after recovery and treatment with anti-inflammatory medication, the errors associated with the same airway scanned at different times would vary greatly. This process also works in reverse, such that the underestimation of airway lumen size before bronchoconstriction will be larger than the underestimation error associated with the same airway measured after constriction, so that the absolute change in lumen area would be underestimated.

In the present study we have developed a software standard, and not a hardware standard. We have created a dataset of micro-CT and HRCT images that we can provide to other researchers to analyse using their different segmentation software. This is not a hardware comparison tool for different CT scanners. In order to make this method applicable to other scanners a better, longer lasting method for preserving the lung tissue samples after they are fixed needs to be developed so that the lung cubes could be sent to different research sites to be scanned by different scanners. The paraffin wax we used to seal the cubes is air permeable, and we found that after a number of weeks the tissue had shrunk noticeably when the cubes were scanned again.

In summary, we have used micro-CT as the standard to calibrate and then measure the accuracy of our current computerised segmentation algorithm for measuring Ai, Aaw and Vi from HRCT. The importance of this work is having a three-dimensional standard for calibration which allows more accurate *in vivo* measurements of airway dimensions from HRCT. This will allow clinicians and researchers to better assess airway pathophysiology. The micro-CT method is more technically complex and only available in large academic centres but its value clearly is as a three-dimensional calibration standard which allows comparison of different models of CT scanners, reconstruction methods and segmentation algorithms. We confirmed that our segmentation algorithm which utilized a radial-spike method underestimated Ai and overestimated Aaw in a size dependent manner, which is in keeping with results of ours and others' previous studies. Having an unbiased 3-dimensional method will allow us to obtain important data on airway lengths, lumen areas and wall areas that are useful for example in modelling studies and in longitudinal treatment studies. The close agreement between morphometry and micro-CT measurements suggests that the two methods are comparable for use as two-dimensional standards. The ultimate goal is that a standard calibration method can be can be used between research groups to address the differences in airway measurements due to different hardware, scanning methodology and reconstruction and segmentation algorithms.

References

1. Venkatraman, R., R. Raman, B. Raman, R. B. Moss, G. D. Rubin, L. H. Mather, and T. E. Robinson. 2006. Fully automated system for three-dimensional bronchial morphology analysis using volumetric multidetector computed tomography of the chest. *Journal of Digital Imaging* 19(2):132-9.
2. Brown, R. H., C. J. Herold, C. A. Hirshman, E. A. Zerhouni, and W. Mitzner. 1991. In vivo measurements of airway reactivity using high-resolution computed tomography. *American Review of Respiratory Disease* 144(1):208-12.
3. Wood, S. A., E. A. Zerhouni, J. D. Hoford, E. A. Hoffman, and W. Mitzner. 1995. Measurement of three-dimensional lung tree structures by using computed tomography. *J Appl Physiol* 79(5):1687-97.
4. Amirav, I., S. S. Kramer, M. M. Grunstein, and E. A. Hoffman. 1993. Assessment of methacholine-induced airway constriction by ultrafast high-resolution computed tomography. *J Appl Physiol* 75(5):2239-50.
5. Herold, C. J., R. H. Brown, W. Mitzner, J. M. Links, C. A. Hirshman, and E. A. Zerhouni. 1991. Assessment of pulmonary airway reactivity with high-resolution CT. *Radiology* 181(2):369-74.
6. Okazawa, M., N. Muller, A. E. McNamara, S. Child, L. Verburgt, and P. D. Pare. 1996. Human airway narrowing measured using high resolution computed tomography. *Am J Respir Crit Care Med* 154(5):1557-62.
7. Niimi, A., H. Matsumoto, R. Amitani, Y. Nakano, M. Mishima, M. Minakuchi, K. Nishimura, H. Itoh, and T. Izumi. 2000. Airway wall thickness in asthma assessed by computed tomography. Relation to clinical indices. *Am J Respir Crit Care Med* 162(4 Pt 1):1518-23.
8. King, G. G., N. L. Muller, K. P. Whittall, Q. S. Xiang, and P. D. Pare. 2000. An analysis algorithm for measuring airway lumen and wall areas from high-resolution computed tomographic data. *Am J Respir Crit Care Med* 161(2 Pt 1):574-80.
9. Goris, M. L., H. J. Zhu, F. G. Blankenberg, F. Chan, and T. E. Robinson. 2003. An automated approach to quantitative air trapping measurements in mild CF lung disease. *Chest* 123:1655-1663.
10. McNitt-Gray, M. F., J. G. Goldin, T. D. Johnson, D. P. Tashkin, and D. R. Aberle. 1997. Development and testing of image-processing methods for the quantitative assessment of airway hyperresponsiveness from high-resolution CT images. *Journal of Computer Assisted Tomography* 21(6):939-47.
11. McNamara, A. E., N. L. Muller, M. Okazawa, J. Arntorp, B. R. Wiggs, and P. D. Pare. 1992. Airway narrowing in excised canine lungs measured by high-resolution computed tomography. *Journal of Applied Physiology* 73(1):307-16.
12. Reinhardt, J. M., N. D. D'Souza, and E. A. Hoffman. 1997. Accurate measurement of intrathoracic airways. *IEEE Transactions on Medical Imaging* 16(6):820-7.
13. Nakano, Y. 2002. Development and validation of human airway analysis algorithm using multidetector row CT. *Proceeding of SPIE. Medical Imaging 2002: Physiology and Function from Multidimensional Images* 4683:460-469.
14. Gevenois, P. A., M. C. Koob, D. Jacobovitz, P. De Vuyst, J. C. Yernault, and J. Struyven. 1993. Whole lung sections for computed tomographic-pathologic correlations. Modified Gough-Wentworth technique. *Invest Radiol* 28(3):242-6.
15. Wiebel, E. R., and R. A. Vidone. 1961. Fixation of the lung by formalin steam in a controlled state of air inflation. *Am Rev Respir Dis* 84:856-861.

16. King, G. G., J. D. Carroll, N. L. Muller, K. P. Whittall, M. Gao, Y. Nakano, and P. D. Pare. 2004. Heterogeneity of narrowing in normal and asthmatic airways measured by HRCT. *Eur Respir J* 24(2):211-8.
17. Bland, J. M., and D. G. Altman. 1996. Measurement error. *Bmj* 313(7059):744.
18. Bland, J. M., and D. G. Altman. 1986. Statistical methods for assessing agreement between two methods of clinical measurement. Lancet 1(8476):307-10.
19. King, G. G., N. L. Muller, and P. D. Pare. 1999. Evaluation of airways in obstructive pulmonary disease using high- resolution computed tomography. Am J Respir Crit Care Med 159(3):992-1004.
20. Saba, O. I., E. A. Hoffman, and J. M. Reinhardt. 2003. Maximizing quantitative accuracy of lung airway lumen and wall measures obtained from X-ray CT imaging. J Appl Physiol 95(3):1063-75.
21. Brown, R. H., P. Croisille, B. Mudge, F. B. Diemer, S. Permutt, and A. Togias. 2000. Airway narrowing in healthy humans inhaling methacholine without deep inspirations demonstrated by HRCT. American Journal of Respiratory & Critical Care Medicine 161(4 Pt 1):1256-63.
22. Bankier, A. A., D. Fleischmann, R. Mallek, A. Windisch, F. W. Winkelbauer, M. Kontrus, L. Havelec, C. J. Herold, and P. Hubsch. 1996. Bronchial wall thickness: appropriate window settings for thin-section CT and radiologic-anatomic correlation. Radiology 199(3):831-6.

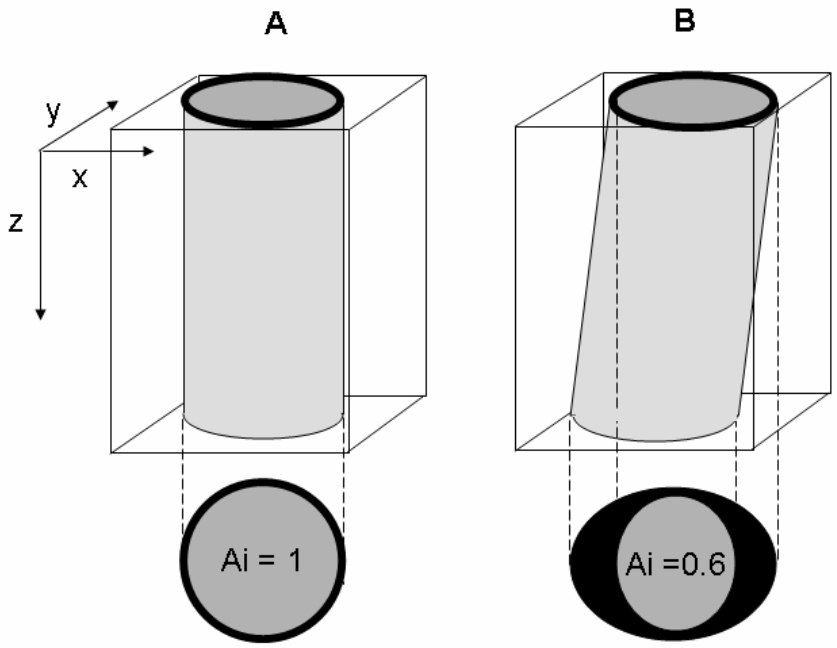

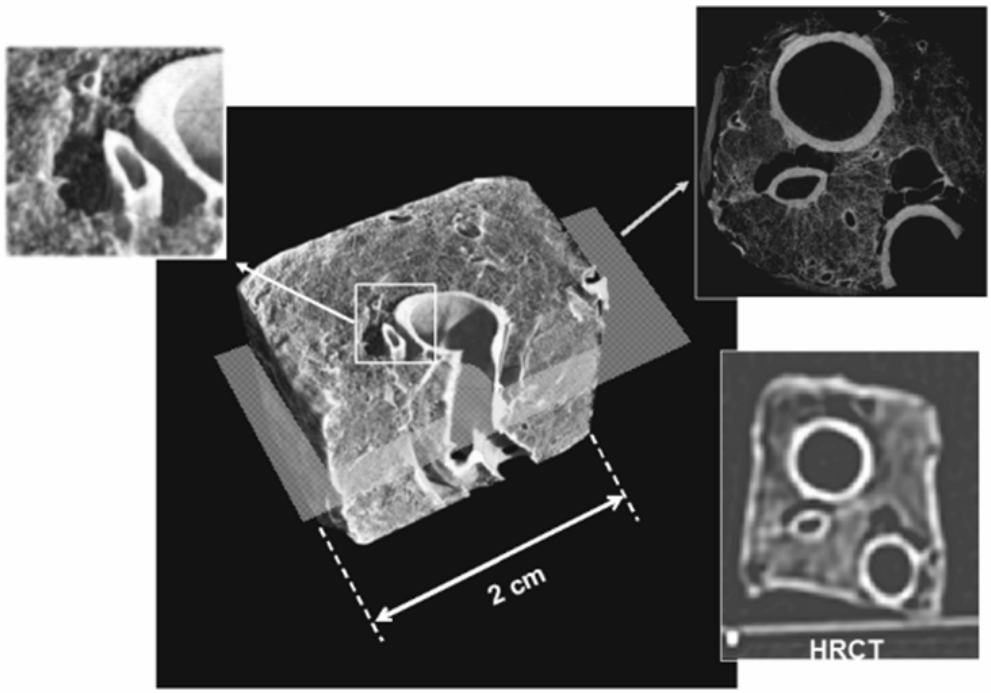
2 cm
HRCT

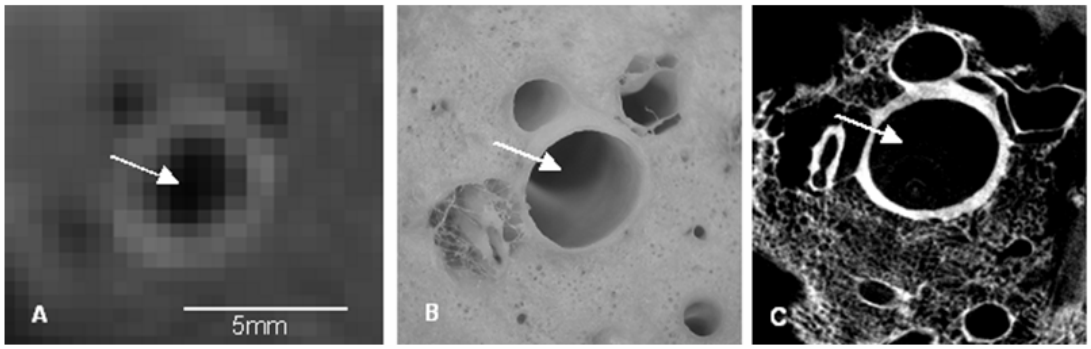
A
5mm
B
C

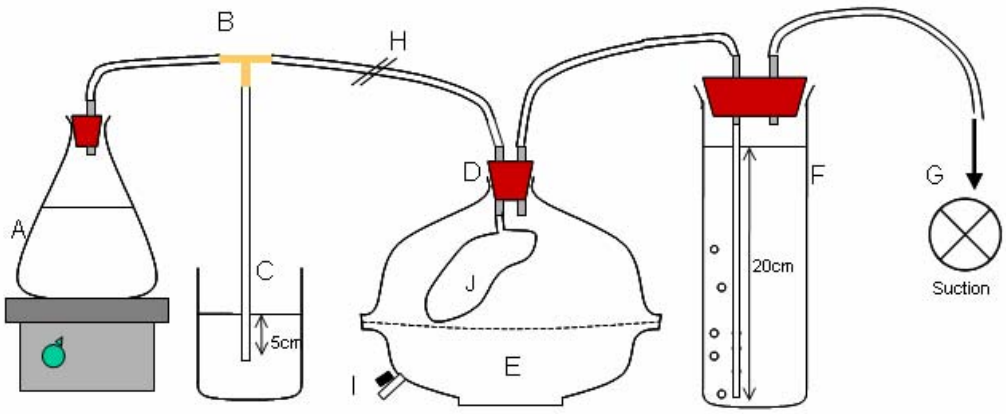
B
H
A
C
5cm
D
J
E
I
F
20cm
G
Suction

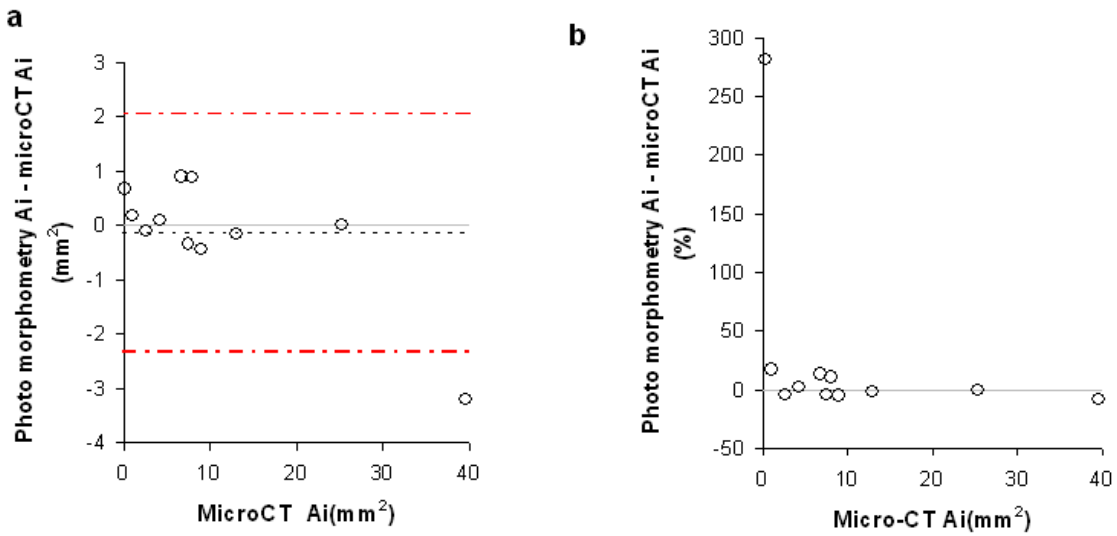
a
Photo morphometry Ai - microCT Ai (mm²)
MicroCT Ai(mm²)
b
Photo morphometry Ai - microCT Ai (%)
Micro-CT Ai(mm²)

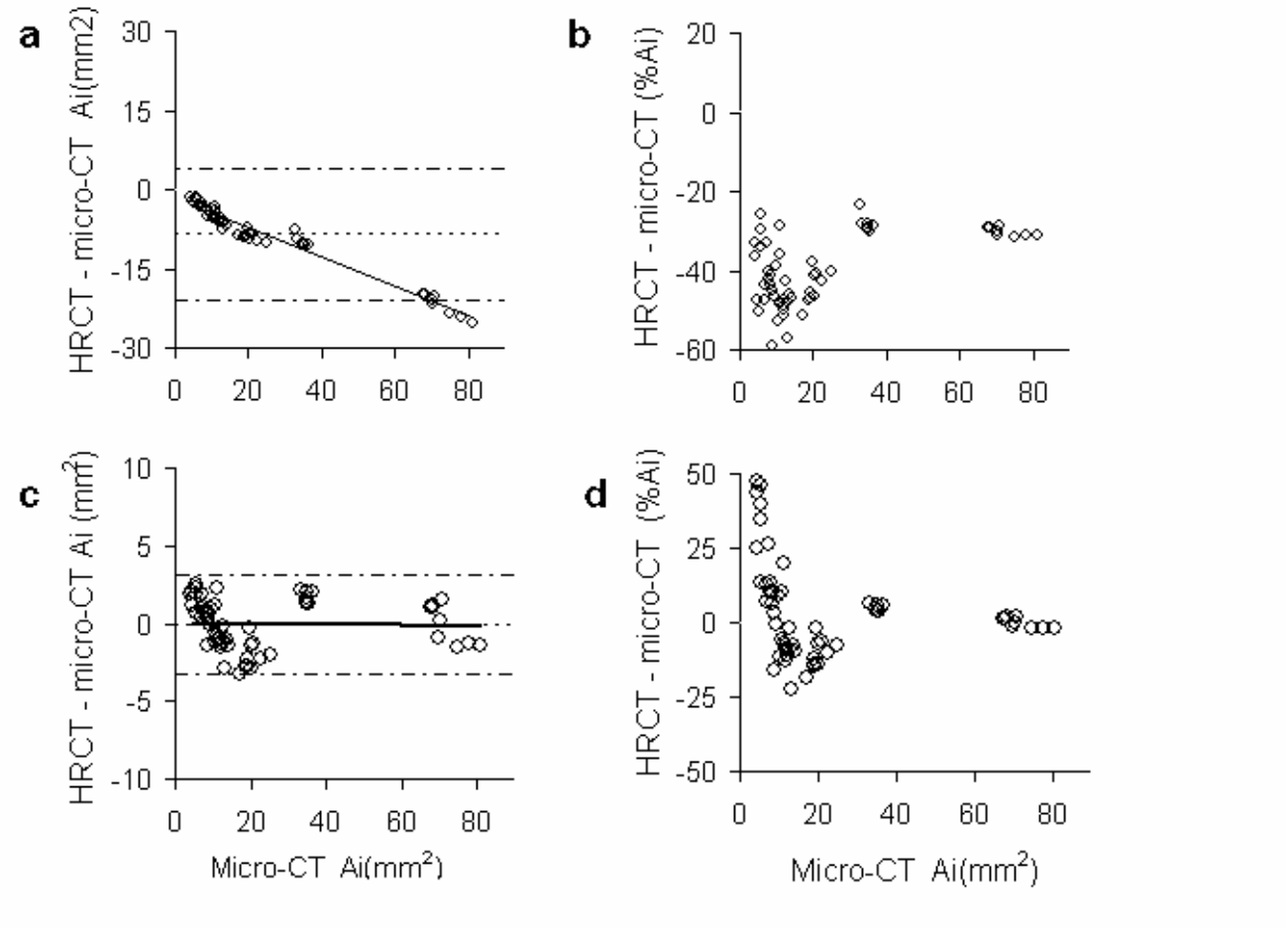
a
HRCT - micro-CT Ai(mm2)
b
HRCT - micro-CT (%Ai)
c
HRCT - micro-CT Ai (mm²)
Micro-CT Ai(mm²)
d
HRCT - micro-CT (%Ai)
Micro-CT Ai(mm²)

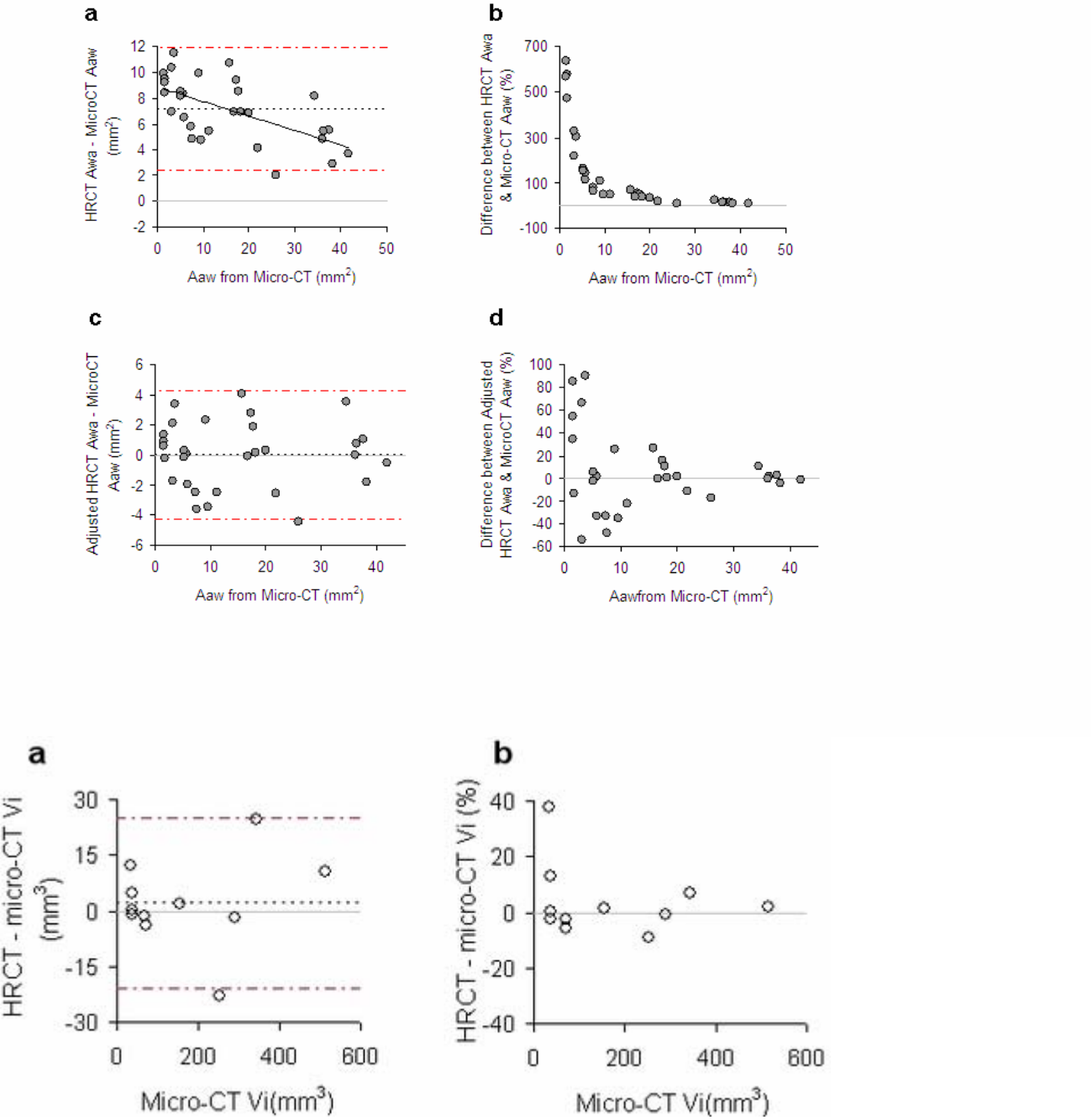
a
HRCT Awa - MicroCT Aaw (mm²)
Aaw from Micro-CT (mm²)
b
Difference between HRCT Awa & Micro-CT Aaw (%)
Aaw from Micro-CT (mm²)
c
Adjusted HRCT Awa - MicroCT Aaw (mm²)
Aaw from Micro-CT (mm²)
d
Difference between Adjusted HRCT Awa & MicroCT Aaw (%)
Aawfrom Micro-CT (mm²)

a
HRCT - micro-CT Vi (mm³)
Micro-CT Vi(mm³)
b
HRCT - micro-CT Vi (%)
Micro-CT Vi(mm³)